Chapter 4
Performance Assessment of Novel Biomass Gasification Based CCHP System integrated with Syngas Production

In this chapter, three novel biomass gasification based tetra-generation systems for syngas, heating, cooling and power generation have been proposed and assessed for selected biomass materials. The systems, instead of using the chemical energy of the gasification products, use the thermal energy to operate a Rankine and Refrigeration cycle in three configurations, namely, steam Rankine cycle with organic Rankine Cycle and ejector refrigeration cycle (Cycle-1), binary Rankine cycle with ejector refrigeration cycle (Cycle-2) and steam Rankine cycle with combined power ejector refrigeration cycle (Cycle-3). Syngas (a mixture of hydrogen and carbon monoxide gas), which has the potential for various domestic applications, has been obtained as the final product. The effects of different operating parameters such as water to biomass ratio, total biomass-water mass flow rate, mass flow rate of refrigerant, generator pressure, gasification temperature and types of biomass material have been studied on the syngas and hydrogen yields, as well as coefficient of performance and overall performance index of the system. The study shows that Cycle-2 is more effective in terms of coefficient of performance and refrigeration effect whereas Cycle-1 is best for higher performance index. Hence, either Cycle-1 or Cycle-2 can be preferred depending on the requirement.

4.1 Model description

The proposed model consists of a biomass gasification unit to produce heat, syngas, as well as power and refrigeration effect. The latter units have been analyzed in three configurations

of heating, power generation and refrigeration systems. Mixing of biomass and water takes place in mixer (M). The mixture is then pressurized to the gasifier unit pressure by pump (P). The gasifier unit of the proposed model consists two aspen reactor blocks: RYIELD and RGIBBS. In Aspen Plus, biomass has been defined as a non-conventional component. Hence, any stream compromised with it must also be considered as a non-conventional mass flow stream. A non-conventional stream must be decomposed into its basic constituents such as C, H_2, O_2, N_2, Cl and S with the help of the RYIELD reactor block for Aspen Plus simulation. For modeling chemical equilibrium at a given temperature and pressure in the RGIBBS reactor block, the principle of minimization of Gibbs free energy has been employed. Since the gasification reactions taking place in the RGIBBS reactor are endothermic in nature, an external source of thermal energy depicted by the heat stream (Q-1) must be supplied into the RGIBBS reactor from RYIELD reactor in order to sustain the gasification process and achieve isothermal conditions in the gasifier. In order to make the gasification process neither endothermic nor exothermic, some amount of air has been introduced into the RGIBBS reactor. The amount of air required ranges from 115.4 kg/h to 517.4 kg/h whereas Q1 lies between 330967 watt to 421775 watt for the biomass materials under consideration. All the three proposed configurations are discussed below.

Cycle -1. Steam Rankine cycle + ORC + ERC

In this configuration, the products formed due to the gasification of biomass in the RGIBBS reactor have been passed through the heat exchanger (HX-1). The steam Rankine cycle is operated via the heat extracted by this heat exchanger as shown in Fig. 4.1. A second heat exchanger (HX-2) has been used for running ORC as the gasification products flow through it. A third heat exchanger (HX-3), which also acts as a boiler, has been employed to operate the ERC.

The ERC has been divided into two parts: Primary and Secondary cycles based on the flow of the working fluid. Boiler generates high pressure and temperature primary vapor which then arrives at the nozzle section of ejector (EJECTOR). The entrainment of secondary vapor from the evaporator into the mixing chamber occurs due to the generation of high vacuum at the entry point of the mixing chamber as the velocity of the vapor at the nozzle exit is very high. In the mixing chamber both the primary and secondary vapor streams get mixed and then the mixed stream goes into the diffuser where its velocity becomes subsonic and it decelerates. A condenser (COND) has been used to condense the stream coming out of the ejector with the help of suitable cooling fluid. The working fluid is then divided in two parts based on the entrainment ratio. One part of the working fluid enters into the throttling valve (VALVE) for expansion after which it flows into the evaporator (EVAPORATOR) whereas the other part flows to the boiler after it has been pressurized by a pump (P-3) to the boiler pressure. The refrigerant at low pressure and temperature inlet into the evaporator has been vaporized as it absorbs latent heat from the water. Thus, the water gets cooled. The refrigerant outlet from the evaporator is in dry state, it then enters into the mixing chamber to complete the secondary cycle. A fourth heat exchanger (HX-4) has been used for minimizing thermal pollution. This has been achieved by the rejection of any remaining thermal energy to the cooling fluid. Lastly, the separation of the gasification products into syngas and other products has been carried out in a separator (SEP). The main assumptions for this cycle have been shown in Table 4.1a.

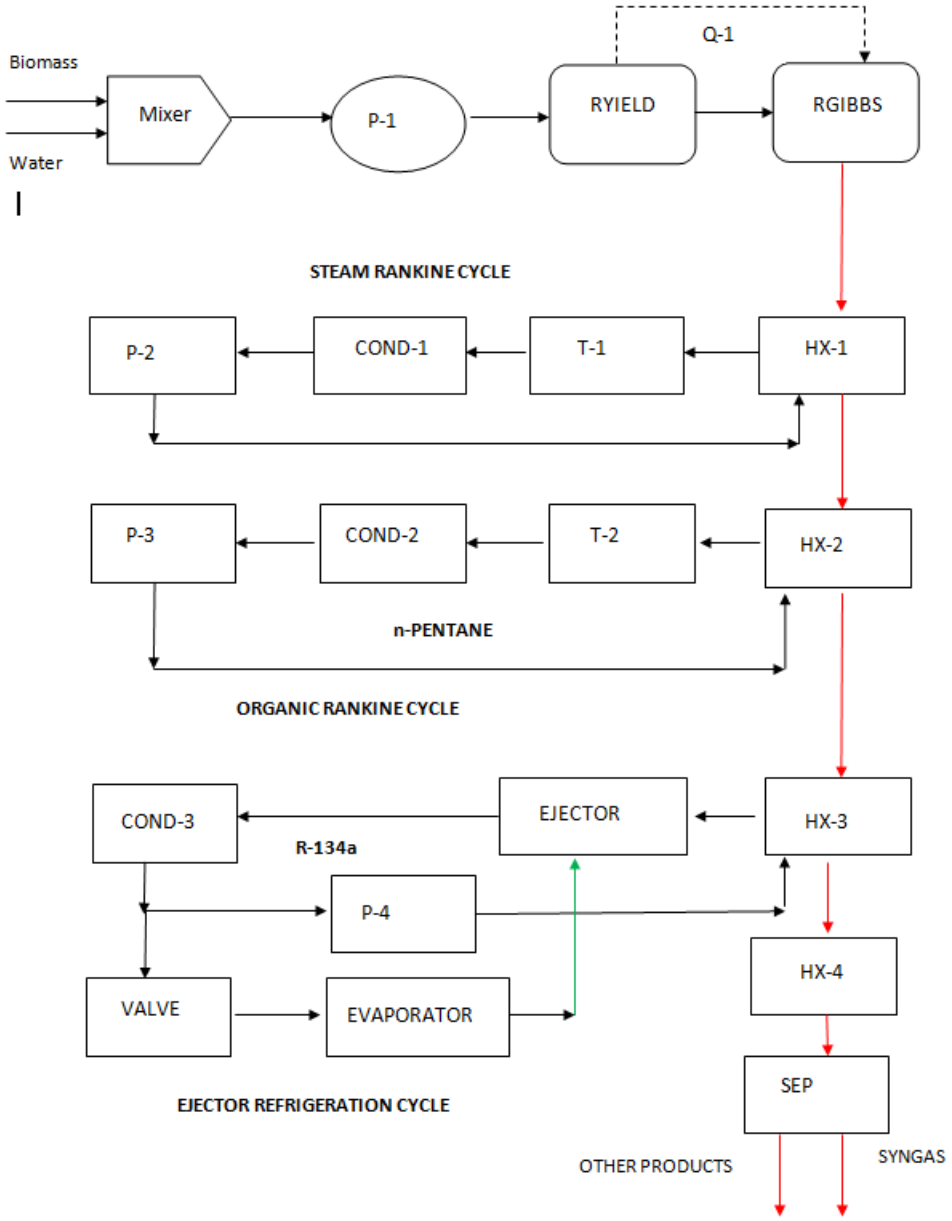

Fig.4.1 Schematic Diagram for Cycle-1

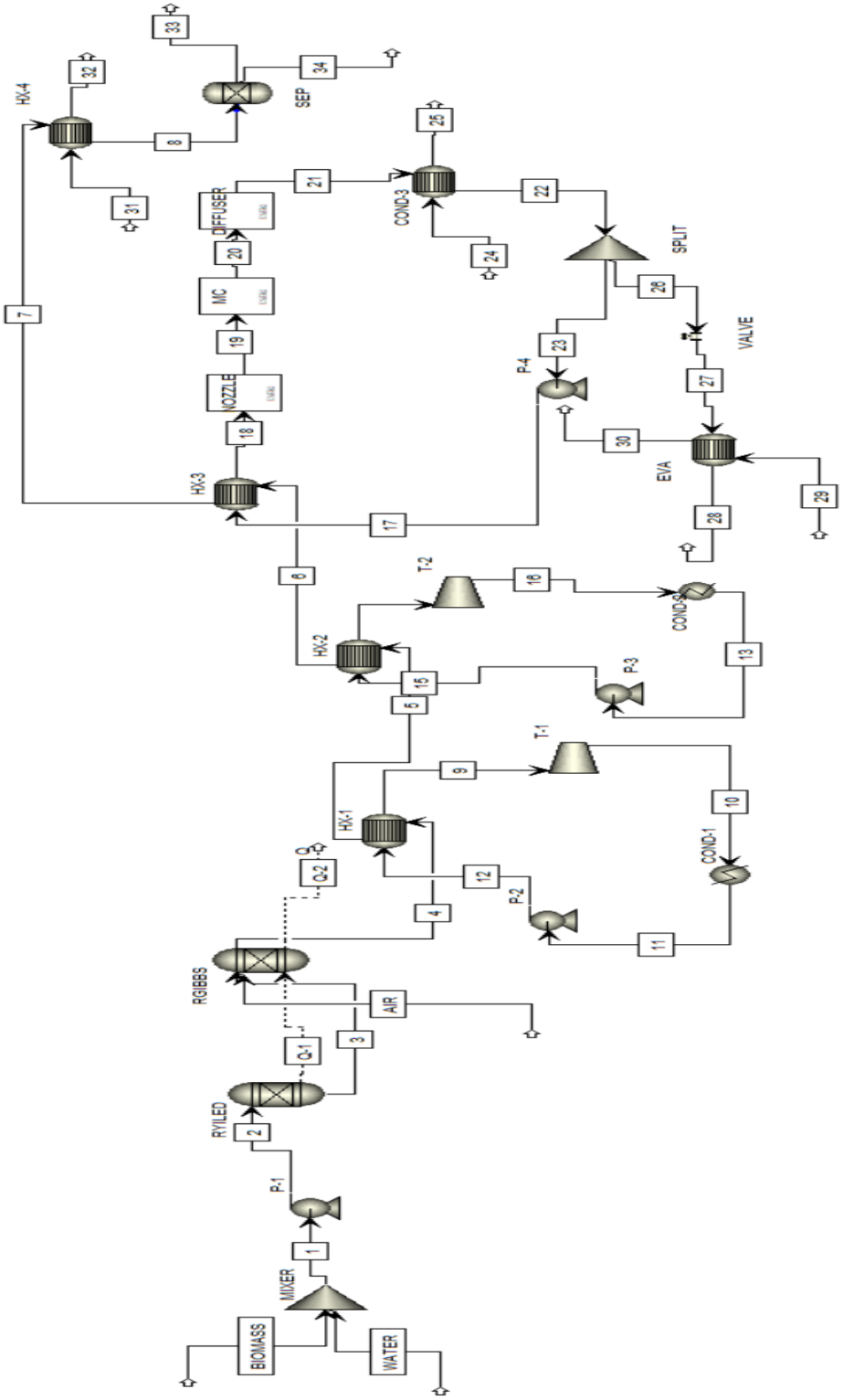

Fig.4.2 Aspen plus flowsheet for cycle-1

Table 4.1a: Main assumptions of Cycle-1

Gasification Unit			
Environment Temperature (K)	300	Condenser Temperature approach (K)	10
Environment Pressure (bar)	1	Turbine outlet pressure (bar)	3
Gasifier Temperature (K)	800-1400	Ejector-refrigeration cycle (R-134a)	
Gasifier Pressure (bar)	1	Heat-exchanger Temp. approach (K)	20
Steam-Rankine cycle (Working Fluid: Water)		Nozzle inlet Pressure(bar)	38
Heat-exchanger Temperature approach (K)	20	Nozzle outlet Pressure(bar)	3.54
Turbine inlet pressure (bar)	100	Mixer chamber Pressure(bar)	3.54
Turbine outlet pressure (bar)	0.4	Condenser Temp. approach (K)	5
Condenser Temp. approach (K)	20	Evaporator Temperature(K)	278
ORC (Working Fluid: n-Pentane)		Water heater outlet temperature(K)	320
Heat-exchanger Temperature approach (K)	20	G-L Separator Temperature(K)	314
Turbine inlet pressure (bar)	20	G-L Separator Pressure(bar)	1
Turbine outlet pressure (bar)	1.2		

Cycle -2. Binary Rankine cycle + ERC

This configuration includes binary vapor power cycle in place of Steam Rankine cycle and ORC. The ERC cycle layout is the same as in Cycle -1. The main assumptions of this configuration have been given in Table 4.1b. As shown in the layout, the mixture of gasification gases discharged from RGIBBS block has been passed through the heat exchanger (HX-1), the binary vapor power cycle has been operated by the use of this heat exchanger as shown in Fig. 4.2. The high temperature and pressure vapor of the primary working fluid (toluene) enters the turbine (T-1) to produce power. After the expansion of the primary working fluid in turbine (T-1), a second heat exchanger (BHX) has been used to change state of the primary working fluid from vapor to saturated liquid. On the other hand, the heat gained by the secondary working fluid causes its phase change from liquid to vapor. This vapor then produces power by running the Turbine (T-2). Finally, the vapor passes through the condenser (COND-1) and again become the saturated liquid. The rest of the setup is same as Cycle -1.

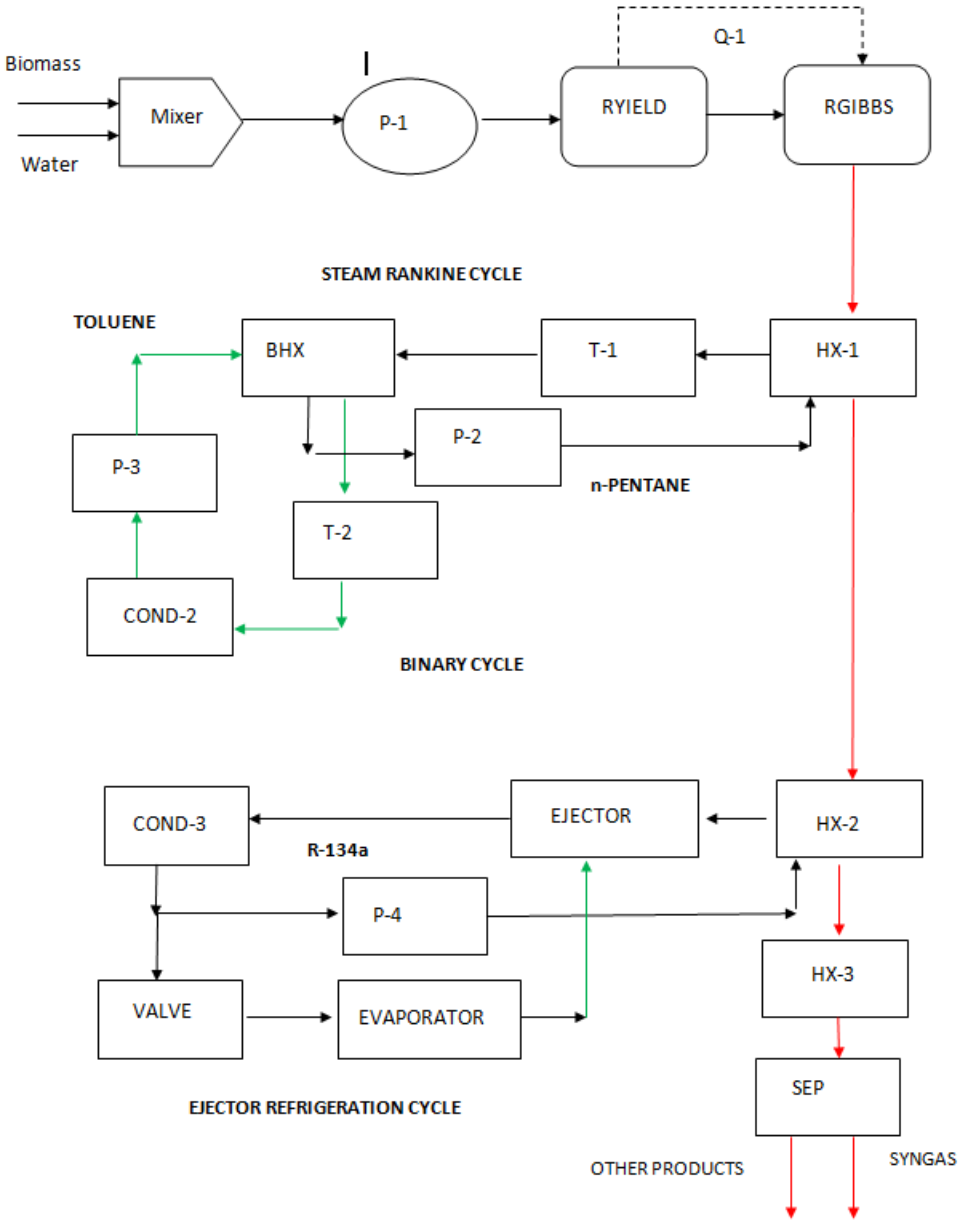

Fig.4.3 Schematic Diagram for Cycle-2

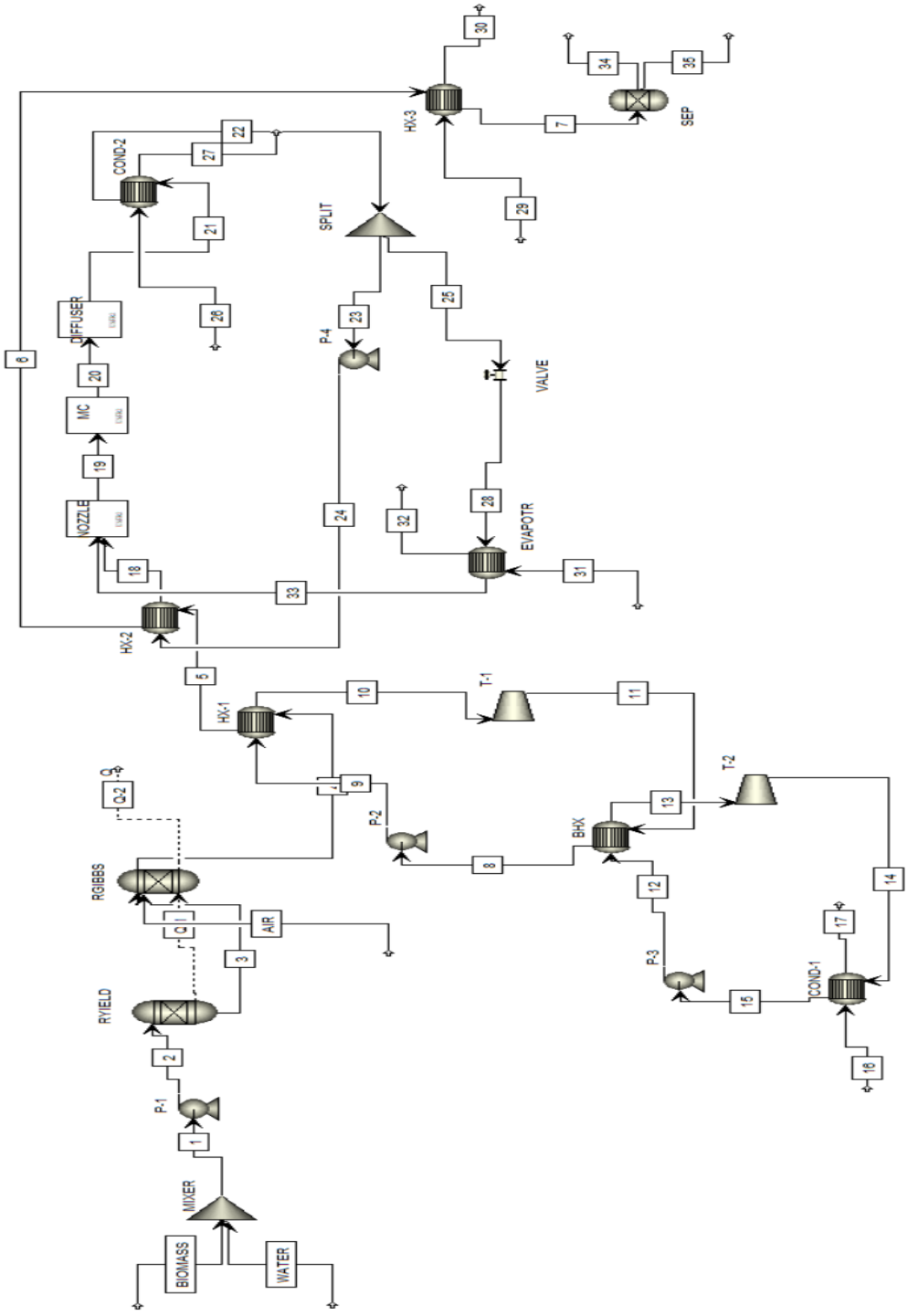

Fig. 4.4 Aspen plus flowsheet for cycle-2

Table 4.1b: Main assumptions of Cycle-2

Gasification Unit		Ejector-refrigeration cycle (R-134a)	
Environment Temperature (K)	300	Heat-exchanger Temp. approach (K)	20
Environment Pressure (bar)	1	Nozzle inlet Pressure(bar)	38
Gasifier Temperature (K)	800-1400	Nozzle outlet Pressure(bar)	3.54
Gasifier Pressure (bar)	1	Mixer chamber Pressure(bar)	3.54
Binary vapor power cycle (Working Fluid: Toluene and n-Pentane)		Condenser Temp. approach (K)	5
Primary cycle (Working Fluid: Toluene)		Evaporator Temperature(K)	278
Heat-exchanger Temp. approach (K)	20	Water heater outlet temperature(K)	320
Turbine inlet pressure (bar)	40	G-L Separator Temperature(K)	314
Turbine outlet pressure (bar)	3	G-L Separator Pressure(bar)	1
Secondary cycle (Working Fluid: n-Pentane)			
Heat-exchanger Temp. approach (K)	20		
Turbine inlet pressure (bar)	12		
Turbine outlet pressure (bar)	1.2		
Condenser Temp. approach (K)	10		

Cycle -3. Steam Rankine cycle + CPERC

This configuration has no separate ORC or ERC; an integrated form of ORC & ERC (CPERC) has been used after the steam Rankine cycle as shown in Fig. 4.3. The turbine (T-2) has been used to expand the high pressure and temperature vapor coming from boiler unit of the

CPERC to produce power. After expansion the vapor then enters the nozzle section of the ejector; the rest of configuration is same as Cycle -1. The main assumptions for this cycle have been presented in Table 4.1c.

Table 4.1c: Main assumptions of Cycle-3

Gasification Unit		Ejector-refrigeration cycle (R-134a)	
Environment Temperature (K)	300	Heat-exchanger Temp. approach (K)	20
Environment Pressure (bar)	1	Turbine Pressure drop (bar)	15
Gasifier Temperature (K)	800-1400	Nozzle inlet Pressure(bar)	38
Gasifier Pressure (bar)	1	Nozzle outlet Pressure(bar)	3.54
Steam-Rankine cycle (Working Fluid: Water)		Mixer chamber Pressure(bar)	3.54
Heat-exchanger Temperature approach (K)	20	Condenser Temp. approach (K)	5
Turbine inlet pressure (bar)	100	Evaporator Temperature(K)	278
Turbine outlet pressure (bar)	0.4	Water heater outlet temperature(K)	320
Condenser Temp. approach (K)	20	G-L Separator Temperature(K)	314
		G-L Separator Pressure(bar)	1

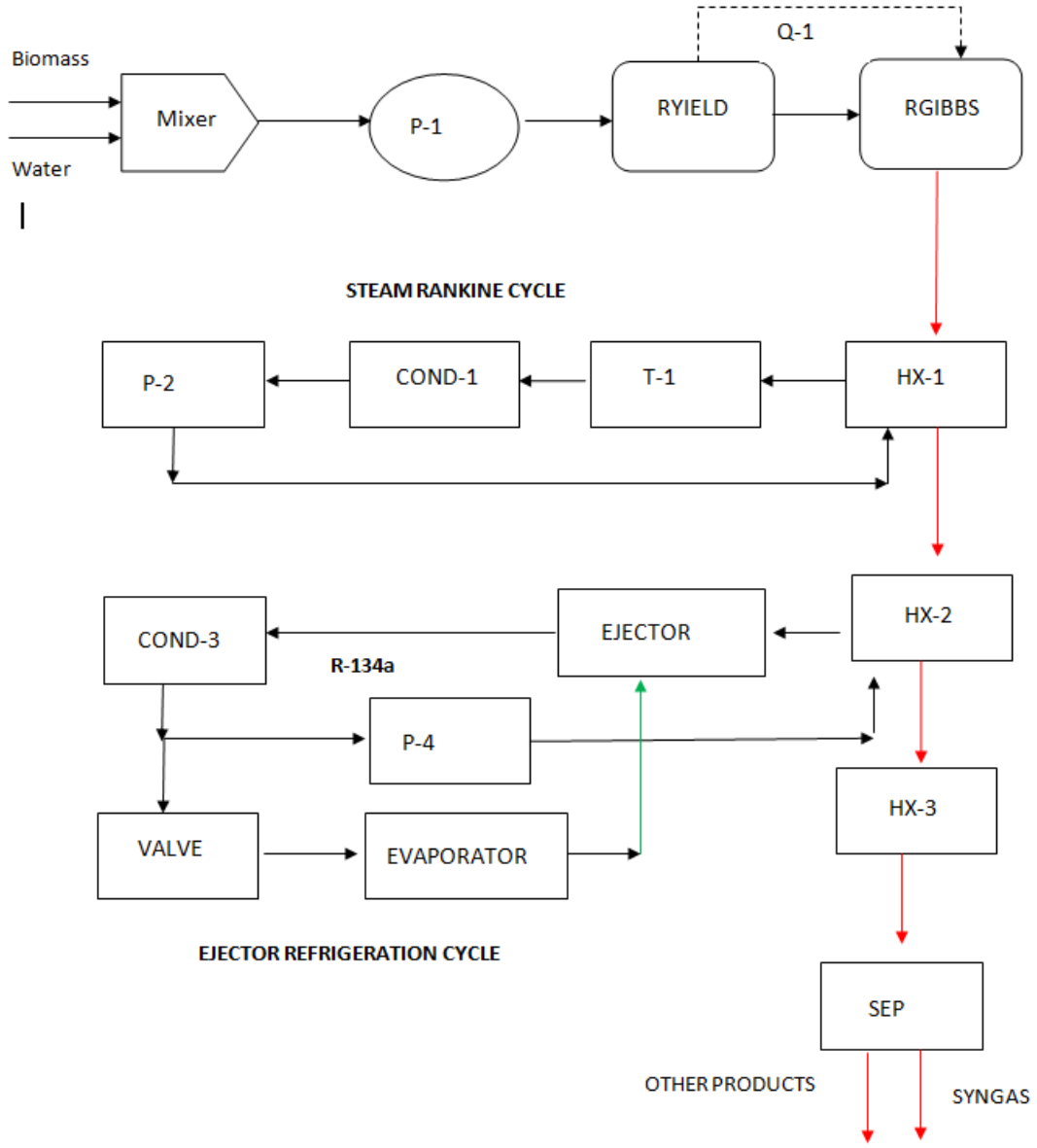

Fig.4.5 Schematic Diagram of Cycle-3

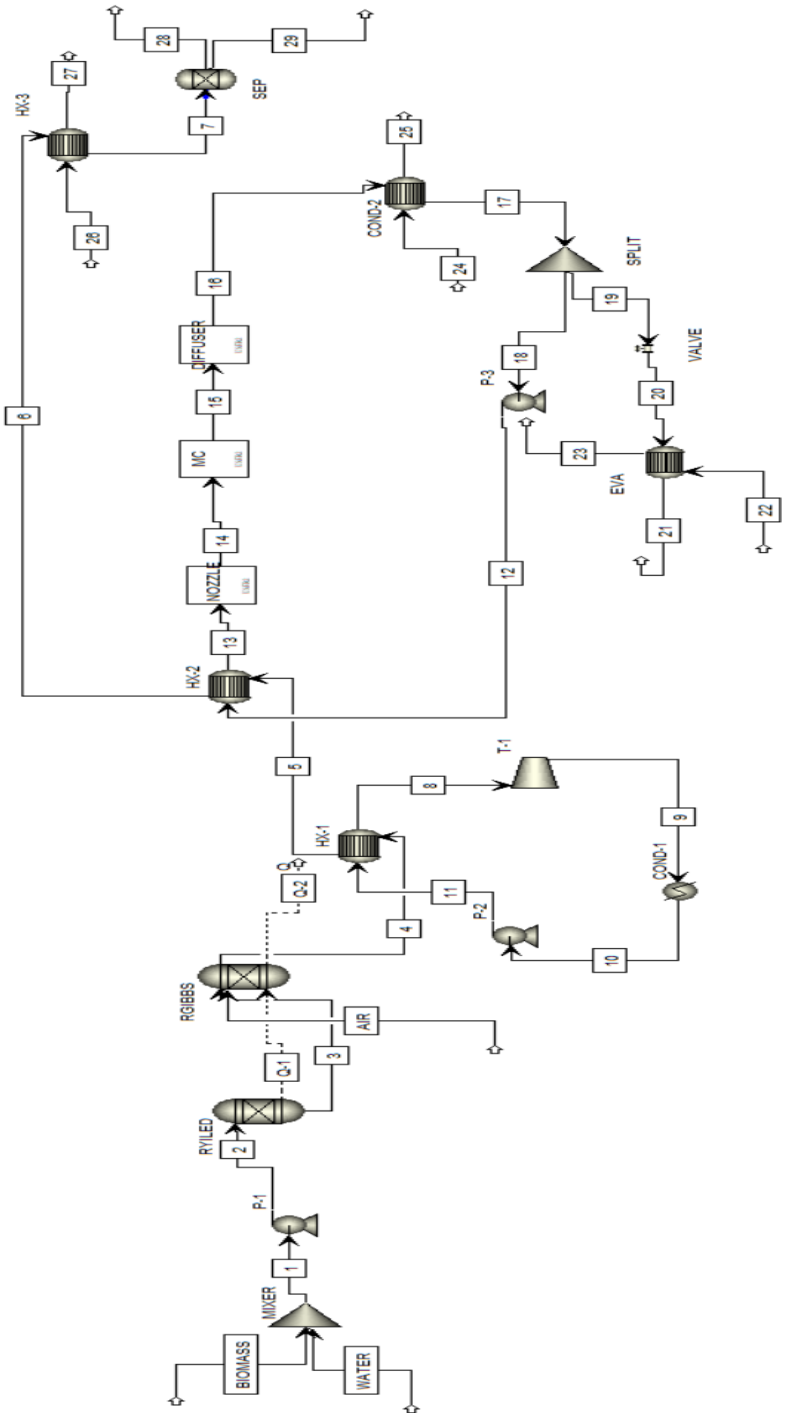

Fig.4.6 Aspen plus flowsheet of Cycle-3

4.2 Mathematical modeling and simulation

The analysis of proposed cycles has been based on the energy balance of each component. For the modeling of the proposed system the following assumptions have been considered (Dai et al., 2009, Prakash et al., 2017):

1. Steady state has been achieved and the heat exchanges with the surroundings are neglected.
2. The Ultimate analysis of the biomass materials considered in the simulation has been taken on dry, ash-free basis (daf), from published literature.
3. Reaction of sulfur has not been considered in the gasification model.
4. Devolatilization of biomass happens instantaneously and volatile products mainly consist of H_2O, H_2, CO, CO_2, CH_4, C_2H_6, N_2, NO_2, NO, NH_3 and O_2.
5. Catalytic effect of char has not been considered in the model.
6. The working fluid in Rankine cycle is saturated liquid when it enters the pump.
7. Sufficient amount of cooling water has been assumed to be available and sink temperature for the model has been taken as 30^oC
8. For this simulation the isentropic efficiencies of turbine and pump have been taken as 0.9 to include losses.
9. In all the heat exchangers, heat transfer takes place under isobaric conditions.
10. Heat exchanger modeling has been done by pinch point temperature approach.
11. The flow through the throttle valve has been considered as isenthalpic.
12. The refrigerant state at the condenser outlet has been assumed to be saturated liquid.

13. The temperature of the refrigerant at condenser outlet has been assumed to be above 308 K in the simulation.
14. At the evaporator exit, the refrigerant has been found to be in dry state.
15. The flow inside the ejector has been assumed to be in steady state and one dimensional for simplicity.
16. The inlet and outlet velocity of refrigerant for the ejector has been assumed to be negligible.
17. The nozzle efficiency, the mixing efficiency and the diffuser efficiency have been used to consider the effects of losses due to friction and mixing in the nozzle, diffuser and mixing chamber. For cycle simulations, the efficiencies of the nozzle, mixer and diffuser have been taken as 0.9, 0.85 and 0.85 respectively.
18. The pressure inside mixing chamber of the ejector operates has been assumed to be constant
19. During the mixing process, laws of conservation of energy and momentum hold.
20. No heat transfer takes place between ejector and environment.

The gasifying agent used is water. At equilibrium condition, C(s), CO, H_2, CO_2, H_2O and CH_4 are the only components which are assumed to be present. The global gasification reaction based on the above assumptions can be written as (Ravikiran et al., 2012) shown in Eq.3.1

For modeling of the proposed system at equilibrium condition, the principle of minimization of Gibbs free energy has been utilized. At equilibrium, total Gibbs free energy (G^t) is dependent on temperature, pressure and the number of moles of i^{th} component (n_i), it can also be written as shown in Eq. 3.2. At equilibrium condition, the total Gibbs free energy will be minimum, i.e., $dG^t = 0$. The rest of the equations are depicted from Eq.3.3 to 3.11

Most researchers analyzed ejector refrigeration systems on the basis of one-dimensional constant pressure flow model (Prakash et al., 2014). So, the ejector simulation has been carried out in this study by using the same approach, adopted by Huang et al., 1999 and Ouzzane et al., 2003.

The ejector has three components namely, nozzle, mixing chamber and diffuser. In the nozzle, the steady flow energy equation for the adiabatic primary flow is given by:

$$h_{n1} = h_{n2} + (u_{n2}^2)/2 \tag{4.1}$$

The nozzle efficiency is given as:

$$\eta_n = (h_{n1} - h_{n2})/(h_{n1} - h_{n2,s}) \tag{4.2}$$

According to Eqs. (4.1) and (4.2), the outlet velocity of primary flow is expressed as:

$$u_{n2} = \sqrt{2\eta_n (h_{n1} - h_{n2,s})} \tag{4.3}$$

The entrainment ratio of the ejector is given as:

$$\mu = m_{sf}/m_{pf} \tag{4.4}$$

Applying the momentum conservation equation in the mixing section, the following relation has been obtained:

$$m_{n2}\, u_{n2} + m_{n3}\, u_{n3} = (m_{n2} + m_{n3})\, u_{n4,s} \tag{4.5}$$

The velocity of secondary flow (u_{n3}) is negligible when compared to the primary flow velocity (u_{n2}), hence Eq. (4.5) becomes:

$$m_{n2}\, u_{n2} = (m_{n2} + m_{n3})\, u_{n4,s} \tag{4.6}$$

From Eqs. (4.4) and (4.6) the following expression has been obtained as:

$$u_{n4,s} = u_{n2}/(1+\mu) \tag{4.7}$$

The mixing efficiency is defined as follows:

$$\eta_m = u_{n4}^2/u_{n4,s}^2 \tag{4.8}$$

Therefore, Eq. (4.7) becomes:

$$u_{n4} = \sqrt{\eta_m}\ u_{n2}/(1+\mu) \tag{4.9}$$

The energy conservation equation for the mixing section is as follows:

$$m_{n2}\,(h_{n2} + u_{n2}^2/2) + m_{n3}\,(h_{n3} + u_{n3}^2/2) = (m_{n2} + m_{n3})(h_{n4} + u_{n4}^2/2) \tag{4.10}$$

Solving Eq. (4.10) for enthalpy at outlet of mixing chamber (h_{n4}) using Eq. (4.4) the following relation has been found as:

$$h_{n4} = (h_{n1} + \mu h_{n3})/(1+\mu) - u_{n4}^2/2 \tag{4.11}$$

For diffuser portion, the mixed fluid converts its kinetic energy into pressure energy; the energy equation for the diffuser section is given as:

$$h_{n4} + u_{n4}^2/2 = h_{n5} + u_{n5}^2/2 \tag{4.12}$$

The diffuser efficiency has been defined as:

$$\eta_d = (h_{n5,s} - h_{n4})/(h_{n5} - h_{n4}) \tag{4.13}$$

In comparison with the inlet velocity of the mixed fluid entering the diffuser (u_{n4}), the outlet velocity of the mixed fluid (u_{n5}) leaving the diffuser is negligible. Therefore, actual enthalpy of the mixed fluid (h_{n5}) at the outlet of the diffuser can be found out as:

$$h_{n5} = h_{n4} + u_{n4}^2/2 \tag{4.14}$$

Using Eq. (24) and Eq.(26), diffuser exit enthalpy has been obtained as:

$$h_{n5} = h_{n4} + (h_{n5,s} - h_{n4})/\eta_d \tag{4.15}$$

Other components of ERC have been modeled based on well-known enthalpy rate balance. The refrigerating or cooling has been calculated based on enthalpy change in evaporator. Then COP for the Cycle-1 and Cycle-2 has been defined as:

$$COP = \frac{Q_{re}}{Q_{in}} \tag{4.16}$$

Where, Q_{re} is the RE and Q_{in} is the heat supplied through the boiler.

The COP of the Cycle-3 has been defined as the ratio of useful energy output and total energy input:

$$COP = \frac{W_{net} + Q_{re}}{Q_{in}} \tag{4.17}$$

Where W_{net} is the net work done by the turbine, Q_{re} is the RE and Q_{in} is the heat supplied through the boiler.

ASPEN PLUS package has been used to carry out the simulation of proposed system based on the above mathematical modeling. Firstly, the evaluation of the outlet condition of the

gasifier has been carried out based on the minimization of Gibbs free energy for a defined set of inlet parameters such as inlet temperature of biomass and water streams (30 ^{0}C), WBR and gasifier pressure (1 bar). Afterwards, the simulation of all the different cycles such as steam Rankine cycle, ORC and ERC utilized in the model has been carried out. The enthalpy balance approach has been used to model each component of Steam Rankine cycle, ORC and ERC; pump and turbine have been modeled based on isentropic efficiency. Minimum temperature approach has been applied for the heat exchanger design (Sarkar et al., 2018). The approach temperature for all the heat exchangers (HX-1, HX-2, HX-3, HX-4) has been taken as 20 K whereas the approach temperatures for various condensers (COND, COND-1) have been taken as 10 K and 5 K, respectively. The various temperature approaches for different heat exchangers used in the proposed system are shown in Tables 4.1a, 4.1b and 4.1c. Turbine and pump employed in the model have been assigned isentropic efficiencies as 0.9 each. Peng-Robinson with Boston-Mathias alpha function (PR-BM) has been adapted as the property method in the proposed model. All the thermodynamic properties were calculated by using the Peng Robinson cubic equation of state with the Boston-Mathias alpha function for the PR-BM property method. The results obtained by this property method were in good agreement with the experimental data. The pressure change in Turbine (T-2) has been kept as 15 bar for the Cycle-3.

R-134a has been selected as the refrigerant because it is widely used as a low pressure refrigerant which is also non-toxic, non-flammable and non-corrosive in nature with comparatively lower global warming potential. However, for lower than 40 bar (critical pressure of R-134a) boiler pressure, RE does not exhibit much appreciable variation with gasification temperature for lower mass flow rates of refrigerant and the condenser temperature has also been found to be lower than the desired outlet temperature of 308 K. There are two ways of increasing

the condenser temperature above the desired level, one is by increasing the boiler pressure and the other one is by decreasing the entrainment ratio. By adopting the second method the RE will decrease, as the mass flow rate in evaporator will decrease when entrainment ratio increases, for which this method is not applicable. Therefore, increasing the boiler pressure above 40 bar can be considered as the suitable option. If the first method is used then as the boiler pressure is increased for a fixed condenser temperature at a specific gasification temperature, the entrainment ratio also increases, which leads to rise in RE.

PI has been defined as a new parameter to comment on the efficiency of the model. It is given by,

$$PI = \frac{Heat\ utilized\ (water\ heating) + Total\ power\ produced + RE}{\overset{o}{m}_{fuel} * CV} \tag{4.18}$$

Where $\dot{m}_{fuel}$ is the mass flow rate of biomass as fuel and CV is the calorific value. Hence, the PI has been determined in the simulation.

In this regard it is worthy to mention that a thermodynamic model of a biomass gasification system integrated with the Steam Rankine cycle and ORC was analyzed using the ASPEN PLUS simulation package by Prakash et al., 2017. Ten readily available Indian biomass materials were compared based on syngas and hydrogen production as well as overall PI of the system. Some of these biomass materials such as wheat straw, rice husk, sugarcane baggasse are abundantly available in India and hence can be used for fuel production without affecting food vs fuel debate. However, in the current study two biomass materials namely, leather waste and paper mill sludge cake, out of ten previously selected biomass materials, have been taken into consideration; since leather waste produces maximum amount of syngas whereas paper mill

sludge cake provides higher performance index for the concerned CHP system along with the assumptions considered in the ASPEN model. Both these biomass materials are totally free from food vs fuel debate and therefore can be used for fuel production. Therefore, the performances of only these two biomass materials have been compared in the present study to select the appropriate one. The ultimate analysis of selected biomass materials has been shown in Table 4.2.

The simulation results from the gasification unit of the present model have been compared with experimental results obtained from the SCWG of glycerol (Byrd et al., 2008), corn starch and sawdust mixtures (Antal et al., 2000). The simulation results exhibited very good agreement with the yields obtained from the experimental studies. The ERC of the model has been validated with the equilibrium results of a model proposed by Dai et al., 2009 as illustrated in Table 4.3. The relative errors for all parameters have been found to be below 5%.

Table 4.2: Ultimate analysis of selected biomass materials

Biomass material	C	H	O	N	S	HHV(MJ/kg)
Paper Mill Sludge Cake (PMSC)	34.2	4.7	60.5	0.5	0.1	10
Leather Waste (LW)	52.1	9.0	23.4	13.1	0.9	25.5

Table 4.3: Model validation between present work and Dai et al., 2009

Parameter	Dai et al.	Present Work	Relative Error (%)
Turbine Work (kW)	114.14	114	0.1
Pump Work (kW)	3.45	3.49	1.1
Boiler Load (kW)	1246.96	1228	1.52
Refrigeration Effect (kW)	60.44	57.59	4.7
Thermal Efficiency (%)	13.72	13.9	1.3

4.3 Results and Discussion

The investigation of the proposed model has been carried out for two WBR (0.4 and 0.6), three TMF (100 kg/h, 125 kg/h and 150 kg/h), six boiler pressures (50 bar, 60 bar, 70 bar, 80 bar, 90 bar and 100 bar), three mass flow rates of refrigerant (100 kg/h, 125 kg/h and 160 kg/h) and two biomass materials namely, PMSC and LW (see Table 4.2). Firstly, the temperature of gasification has been optimized for each of the biomass materials and WBR under consideration. The determined optimum gasification temperature produces highest moles of syngas for a given biomass material and WBR. A graphical plot of yield of syngas versus temperature of gasification has been plotted for both PMSC and LW; it has been found that at a certain temperature syngas yields were maximum for both the biomass materials. The behavior of syngas yield with gasification temperature (K) for Paper Mill Sludge Cake (PMSC), under different conditions, has been illustrated by Fig. 4.4. The simulation of the model as well as calculation of the various output parameters such as PI and COP has been performed based on the computed value of the optimum gasification temperature.

4.3.1 Effects of gasification temperature and WBR at constant TMF, boiler pressure and refrigerant flow rate

Fig. 4.4 presents the variation of syngas and hydrogen productions with respect to the gasification temperature. It has been observed that as the gasification temperature increases the syngas yield also increases until maximum syngas production was achieved, this temperature has been as the optimum gasification temperature. Furthermore, the syngas production declined as the gasification temperature was increased beyond the optimum gasification temperature. The optimum gasification temperature, which is different for each biomass, is higher for lower WBR value. A similar trend was also observed for hydrogen gas. Additionally, for gasification temperatures higher than optimum gasification temperature yield of syngas increases as WBR decreases. However, for gasification temperatures lower than the optimum gasification temperature yield of syngas increases as WBR increases (Prakash et al., 2017). This observation holds true for all the three cycles taken in consideration since the gasification product yields does not affect other performance parameters due to same configuration of gasifier part.

RE has been found to be decreased with increasing gasification temperature. RE has been found to be higher for lower WBR for cycle-1 and cycle-3 whereas for cycle-2 both WBR values provide the same effect (Fig. 4.5). The reason for this can be understood with the help of Eqs. 4.4, 4.7 and 4.8. With increasing gasification temperature, the enthalpy at the inlet and outlet of ejector increases, for a constant value of entrainment ratio, which leads to increase in condenser temperature. As condenser temperature rises, its pressure also increases which causes lower RE. The COP also follows the congruent nature of the RE. It increases with lowering of gasification temperature, for higher gasification temperatures COP becomes nearly constant for a particular pressure, as shown in Fig. 4.5. COP decreases as the heat supplied to the cycle becomes higher

whereas RE becomes lower with increase in gasification temperature. As shown in Fig. 4.6, the PI of all the cycles increases as gasification temperature was increased and higher WBR gives higher value of PI. The range of gasification temperatures for the analysis of PI has been taken as 800-1400 K, since the magnitude of PI at lower than 800 K is negligible due to less heat and power generated (Prakash et al., 2017).

4.3.2 Effects of gasification temperature and total biomass-water mass flow rate at fixed water-biomass ratio, boiler pressure and refrigerant flow rate

From the previous results, it is quite clear that low WBR yields high syngas yield. Hence, WBR has been taken as 0.4 for analysis of this case. Syngas and hydrogen gas show similar behavior with gasification temperature, as described previously. Fig. 4.7 shows that more syngas has been produced at higher TMF than at lower TMF. However, the optimum gasification temperature has been found to be independent of TMF. In other words, TMF has no effect on the optimum gasification temperature. The yield of hydrogen gas has been observed to be directly proportional to TMF, as TMF increases hydrogen production also increases as shown in Fig. 4.7.

The RE has been found to be decreasing with gasification temperature until a minimum value was reached as depicted in Fig. 4.8, as discussed in the previous case. The higher values of TMF produced lesser RE than smaller TMF values. This may be due to the fact that higher TMF values causes an increase in enthalpy at the inlet of the ejector due to fixed pinch point design of the heat exchangers used in the model as explained in the previous case and the entrainment ratio decreases, which leads to a lower value of RE. COP increases rapidly as the TMF is decreased showing an inverse relationship. At lower TMF values a sudden increase in the magnitude of COP at less than 925 K has been observed with maximal value at the lowest extreme of the

temperature range taken for Cycle-2, as shown in Fig. 4.8. PI does not depend on TMF (as it is a ratio of different energy parameters) as shown in Fig. 4.9.

4.3.3 Effects of Boiler Pressure, refrigerant flow rate and gasification temperature at constant TMF (160 kg/h) and WBR (0.4)

This case only deals with the analysis of the ERC and other blocks of the model have not been considered here.RE increases with increase in boiler pressure as shown in Fig. 4.10. Maximal value of RE obtained has been found to be greater for higher boiler pressures. It should be noted that RE for Cycle-2 was greater than the other two cycles; Cycle-3 has the least RE. However, for the temperature range lower than 750K-800K RE in cycle-1 is more rather than cycle-2. PI is independent of boiler pressure hence PI remains constant for any boiler pressure as the gasification temperature increases as depicted in Fig. 4.11. At higher refrigerant flow rate, the RE is higher as compared to lower flow rate as shown in Fig. 4.12. A higher refrigerant flow rate means higher quantity of refrigerant present in the system which generates greater RE. COP shows similar trend as RE, with greater boiler pressure giving higher performance than lower boiler pressure, however, it is independent of refrigerant flow rate. Cycle-2 outperforms other two cycles in case of COP. PI is independent of refrigerant mass flow rates as depicted in Fig. 4.13. Cycle-1 and Cycle-2 have comparable PI.

4.3.4 Comparison of various output parameters obtained from Leather waste and Paper Mill Sludge Cake at optimum gasification temperature

The amount of syngas production at optimum gasification temperature is shown in Fig. 4.14. Syngas production has an inverse relationship with WBR for both biomass materials. The yields of syngas for the WBR of 0.4 and 0.6 have been found to be 8995 mol/h and 7235 mol/h,

respectively, for leather waste. Syngas production for LW is significantly higher than PMSC due to higher carbon content in LW. As discussed earlier, syngas production is similar for all the cycles. For the investigation of PI, COP and RE with respect to all the cycles for the selected biomass materials, a bar chart has been prepared at constant WBR value equal to 0.4 (as it generates more syngas and RE). RE is reported to be maximum for Cycle-2 which is just slightly ahead of Cycle-1. It is minimum for Cycle-3 as shown in Fig. 4.15. RE is found to be maximum for Cycle-2 for PMSC. COP of Cycle-2 is greater than other two cycles; Cycle-3 has the least performance as compared to other two cycles as shown in Fig. 4.16. PMSC achieves maximum COP for Cycle-2. The PI of both the biomass materials has been observed to be equal for Cycle-1and Cycle-2 whereas for Cycle-3 it is the lowest as shown in Fig. 4.17. The PI is maximum for PMSC with Cycle-1 (slightly more than Cycle-2).

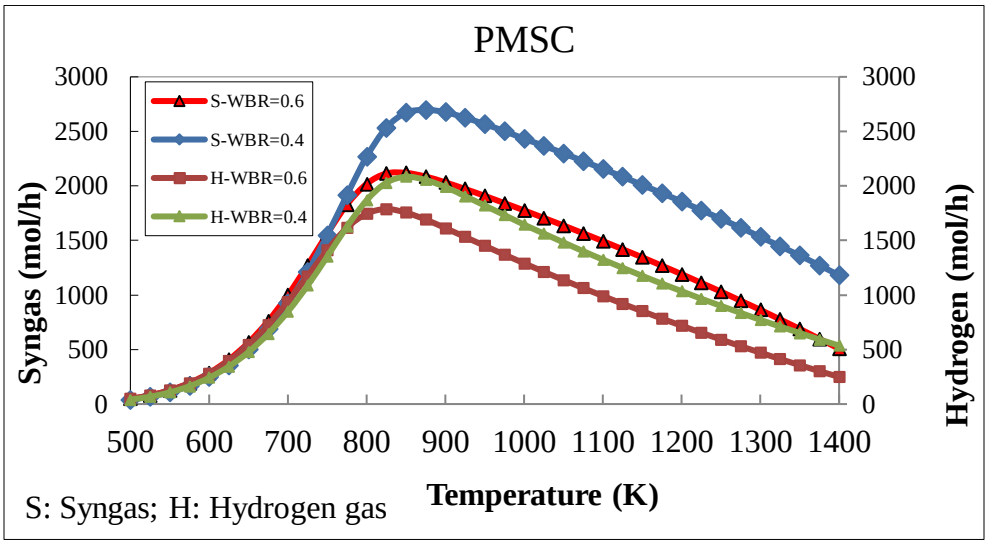

Fig. 4.7 Variations of syngas and hydrogen gas yield with gasification temperature for PMSC with constant TMF (160 kg/h) but with varying WBR

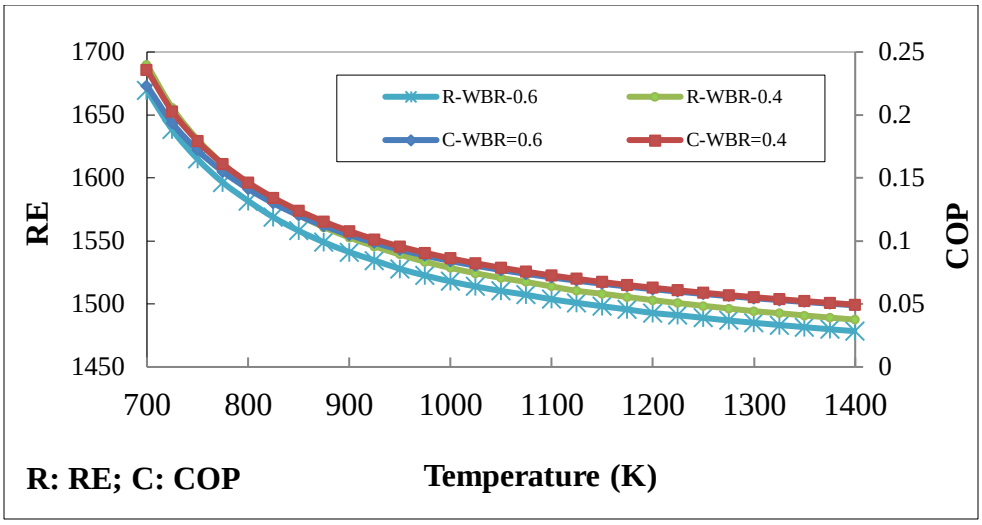

Fig. 4.8 RE and COP vs. gasification temperature with varying water WBR at a fixed boiler pressure (100 bar) and constant TMF (160 kg/h) for Cycle-1

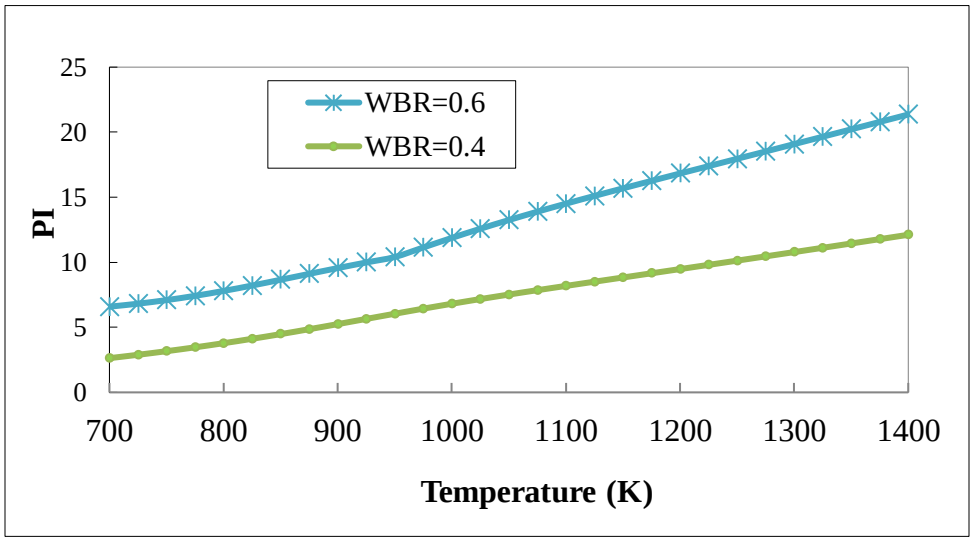

Fig. 4.9 PI vs. gasification temperature with varying WBR at a fixed boiler pressure (100 bar) and constant TMF (160 kg/h) for Cycle-1

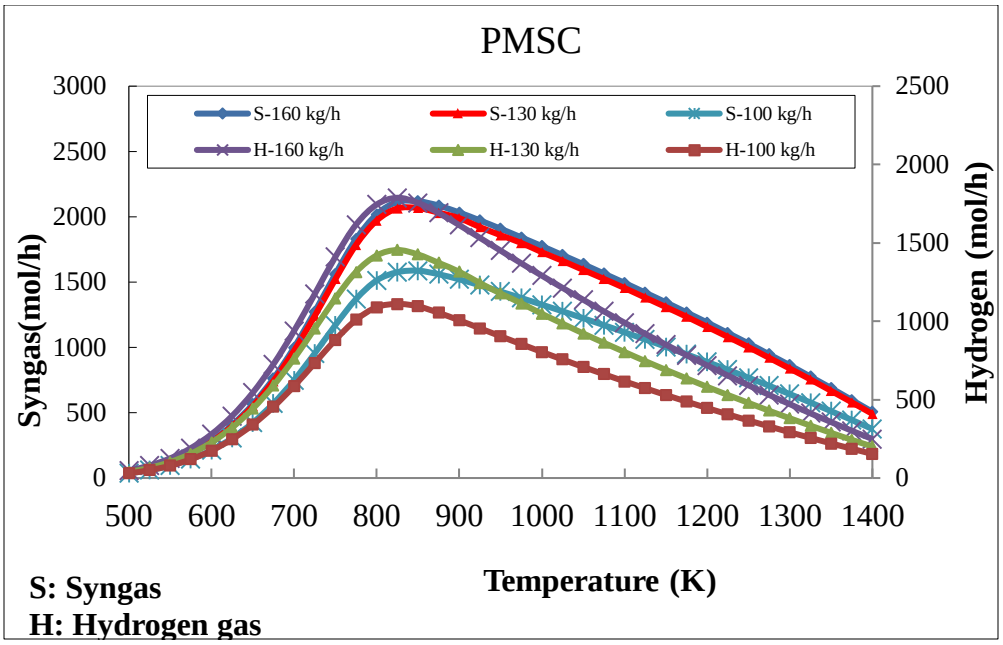

Fig. 4.10 Plot of syngas (mol/h) and hydrogen (mol/h) vs. gasification temperature for PMSC with varying TMF and constant WBR (0.4)

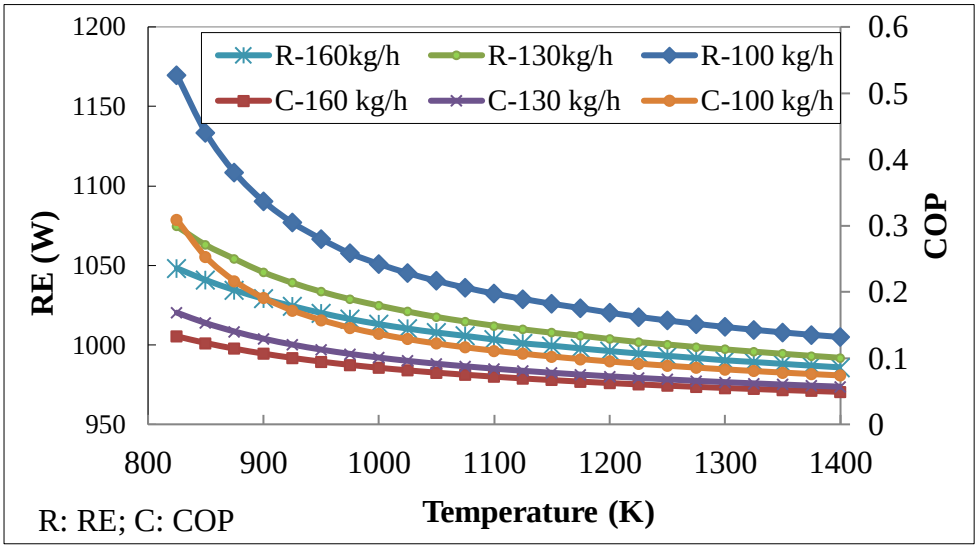

Fig. 4.11 Plot of RE and COP vs. gasification temperature for PMSC with varying TMF at a fixed boiler pressure (100 bar) and WBR (0.4) for Cycle-1

.

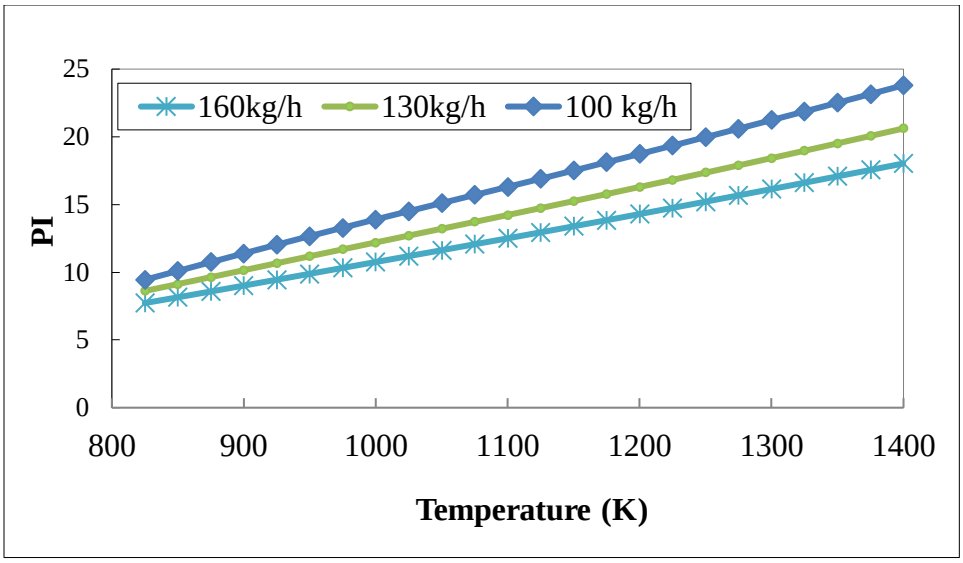

Fig. 4.12 Plot of PI vs. gasification temperature for PMSC with varying TMF at a fixed boiler pressure (100 bar) and constant WBR (0.4) for Cycle-1

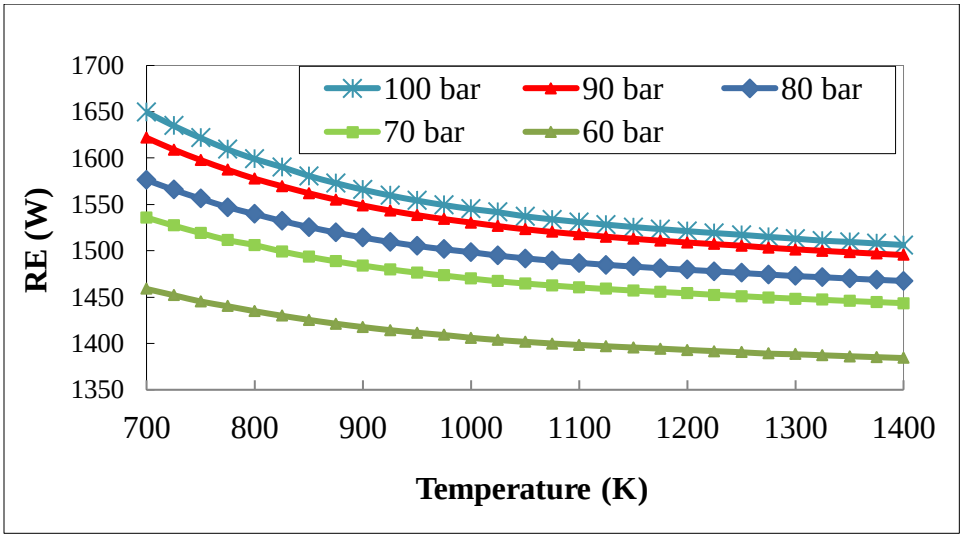

Fig. 4.13 Plot of RE vs. gasification temperature for PMSC with varying boiler pressure at constant TMF (160 kg/h) and WBR (0.4) for Cycle-1

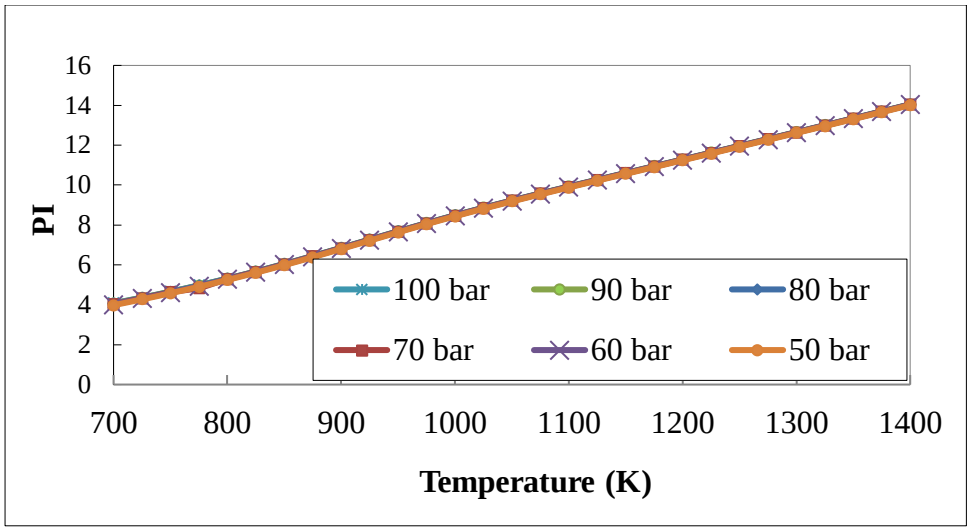

Fig. 4.14 Plot of PI vs. gasification temperature for PMSC with varying boiler pressure at constant TMF (160 kg/h) and WBR (0.4) for Cycle-1

.

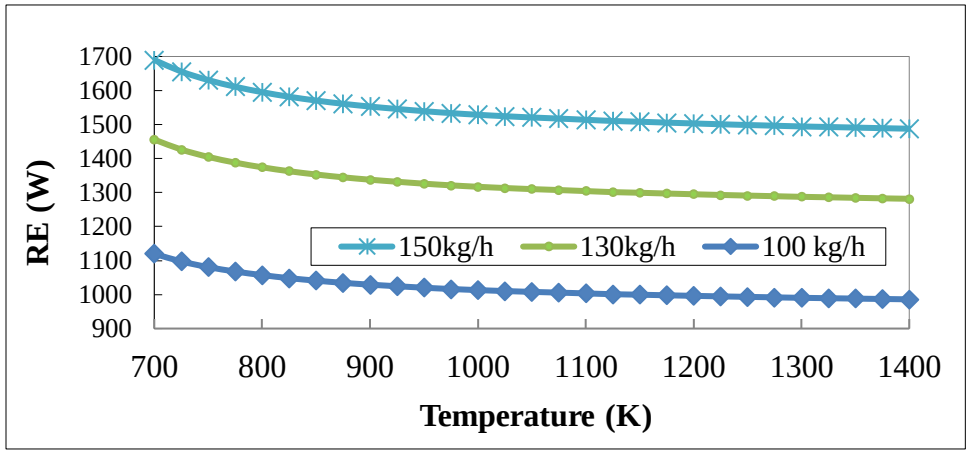

Fig. 4.15 Refrigeration effect vs. gasification temperature for PMSC with varying refrigerant mass flow rate at fixed boiler pressure (100bar), TMF (160 kg/h) and WBR (0.4) for Cycle-1

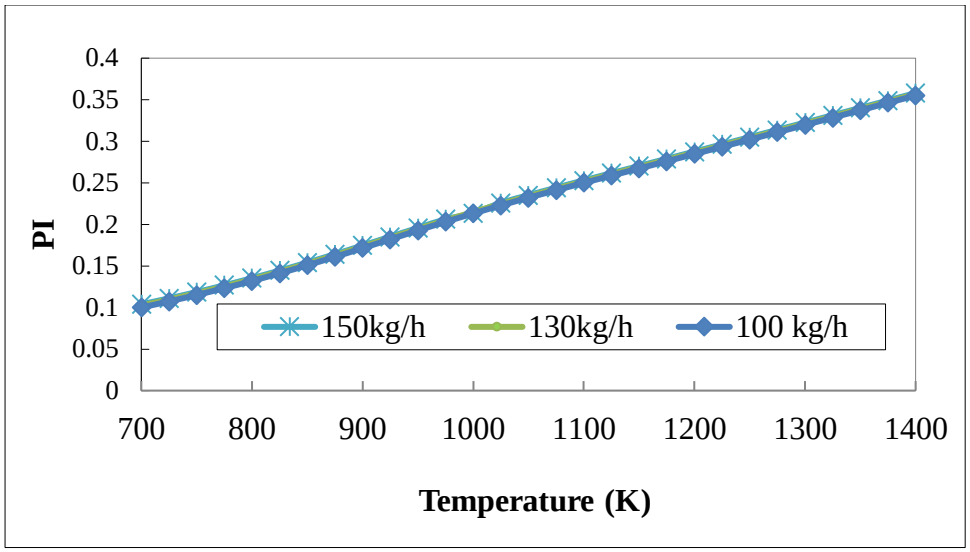

Fig. 4.16 PI vs. gasification temperature for PMSC with varying refrigerant mass flow rate at a fixed boiler pressure (100 bar), TMF (160 kg/h) and WBR (0.4) for Cycle-1

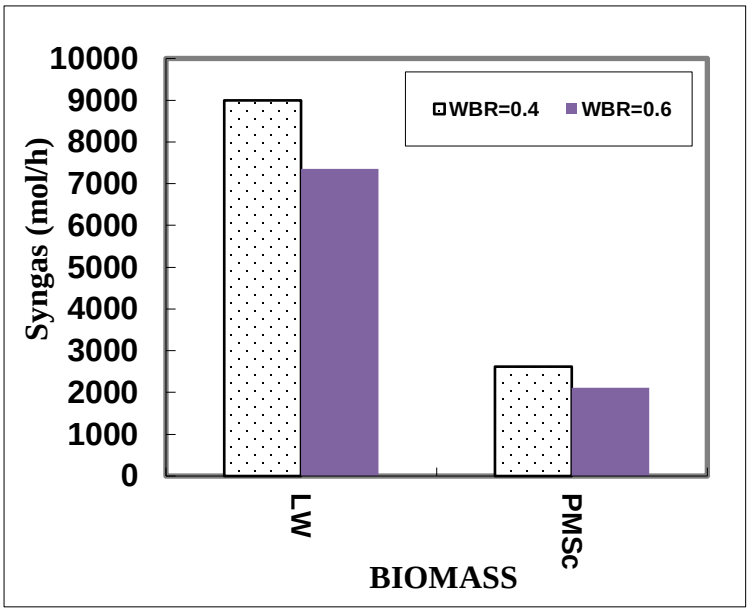

Fig. 4.17 Moles of syngas produced for selected biomass materials with constant total mass flow rate (160 kg/h) and refrigerant flow rate (150 kg/h) at optimum gasification temperature a for all three cycles

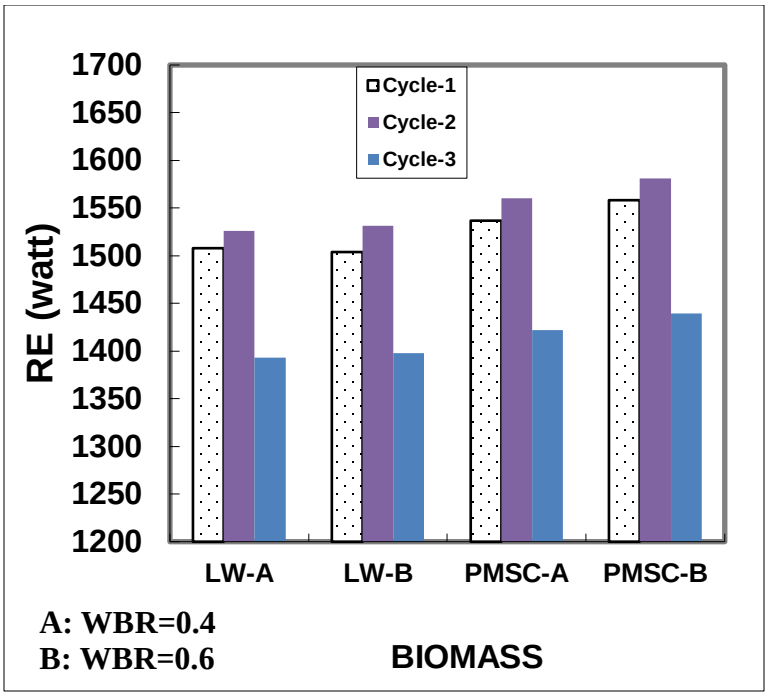

Fig. 4.18 Refrigerant effect for selected biomass materials at different WBR with constant TMF (160 kg/h) and refrigerant flow rate (150 kg/h)at optimum gasification temperature and boiler pressure (100 bar) for all three cycles

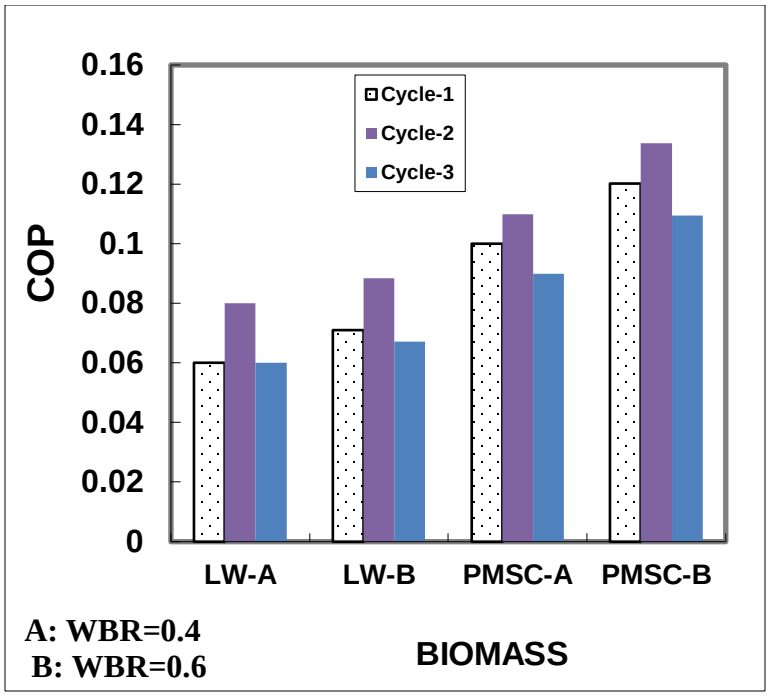

Fig. 4.19 COP for selected biomass materials with constant TMF (160 kg/h) and refrigerant flow rate (150 kg/h) at optimum gasification temperature and boiler pressure (100 bar) for all three cycles

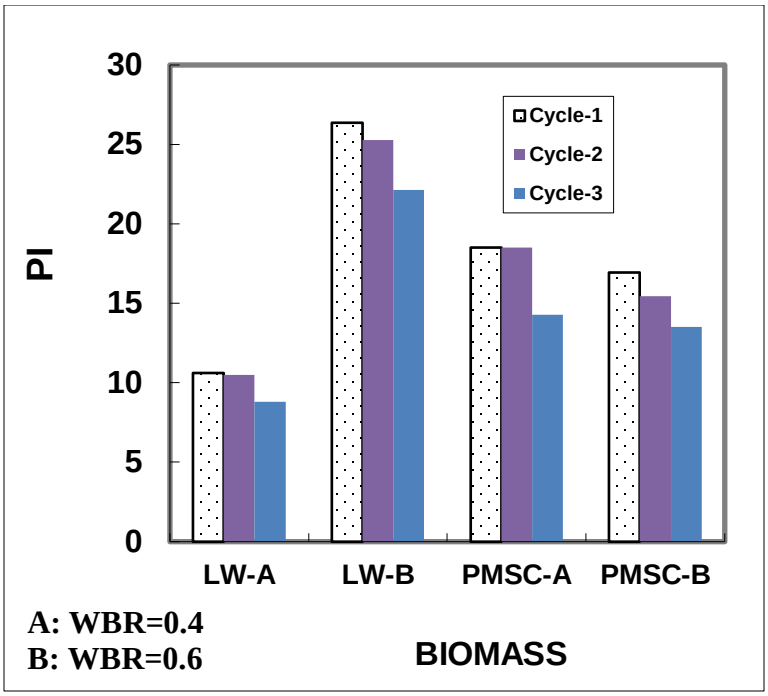

Fig. 4.20 PI for selected biomass materials with constant TMF (160 kg/h) and refrigerant flow rate (150 kg/h) at optimum gasification temperature and boiler pressure (100 bar) for all three cycles